OPTICAL INVESTIGATION OF DUST IN THE SOLAR SYSTEM

R.H. Giese
Ruhr-Universität Bochum, Bereich Extraterrestrische
Physik, Germany

An introduction to definitions and methods used for interpretation of zodiacal light is given together with a short summary of observational results. After this, predictions for probing the zodiacal light by an out of ecliptic space probe and possibilities of explaining the scattering of interplanetary and cometary dust by irregular and fluffy particles are presented.

1. GENERAL SURVEY

1.1 Scope

One method of investigating interplanetary dust is analysis of the zodiacal light (including F-corona and Gegenschein). Since there are extended and excellent reviews available (Leinert 1975, Weinberg and Sparrow 1978) this presentation provides only a short overview which might help to appreciate the papers which follow.

1.2 Definitions

<u>Intensity</u> (surface brightness: erg $cm^{-2}s^{-1}ster^{-1}A^{-1}$) is usually expressed in stars of tenth magnitude (visual) of solar spectral type per square degree (ref. Weinberg and Sparrow 1978), hereafter called S_{10}. If I_1 and I_2 are the intensities of the component with the electric vector perpendicular or parallel to the plane of scattering (Sun, line of sight LOS), respectively, there are 3 quantities usually given for the zodiacal light:

o Total brightness: $I = I_1 + I_2$ (1)

o Polarization:
   either $I_p = I_1 - I_2$,   (polarized component)   (2)

   or $p = (I_1 - I_2)/I$, (degree of polarization)   (3)

1

o   Color ratio:

$$C(\lambda_1, \lambda_2) = \frac{I_{ZL}(\lambda_1)/I_{\odot}(\lambda_1)}{I_{ZL}(\lambda_2)/I_{\odot}(\lambda_2)} \qquad (4)$$

Here λ_1 and λ_2 stand for wavelength and $\odot$ or ZL for Sun or zodiacal light, respectively. If $\lambda_1 < \lambda_2$ reddening of the zodiacal light compared to the solar spectrum results in C < 1.

The <u>viewing direction</u> (LOS, see Figure 1) is defined with respect to the ecliptic plane by ecliptic latitude β and by the difference $L = \ell - \ell_{\odot}$ between the ecliptic longitude of the LOS and the Sun as seen from the observers location (A). These definitions can be transferred even to an observer B (spaceprobe) out of the ecliptic plane as shown in Fig. 1. The angle ε between the direction towards the Sun and the viewing direction is elongation (Fig. 1: ε_A and ε_B).
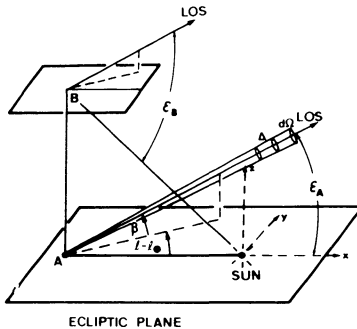

Figure 1
Basic Geometry

The <u>position</u> in the solar system will be defined in a heliocentric coordinate system (Fig. 1: X, Y, Z). Location of the spacecraft is written in capitals and $R = (X^2 + Y^2 + Z^2)^{\frac{1}{2}}$. Positions of dust will be given by x, y, z or $r = (x^2 + y^2 + z^2)^{\frac{1}{2}}$ and $z = r \sin \beta_{\odot}$, where $\beta_{\odot}$ is the heliocentric ecliptic latitude of the position vector $\vec{r}$.

1.3   Observations near 1 AU (Earth)

The reviews referred to above compare the results of many observers for I, P and C as a function of ε in the ecliptic plane.

There is a deep decrease in the intensity I ~ $\varepsilon^{-2.2}$ from the Sun to ε ≃ 45°, followed by a shallow minimum in the region 120° ≤ ε ≤ 150° and by an increase of about 30 to 50 S_{10} from ε ≃ 160° towards ε = 180° (Gegenschein). The degree of polarization is mainly positive with a maximum of P ≃ 0.17 to 0.23 in the region 60° ≤ ε ≤ 80°. Several workers found a polarization reversal and slightly negative polarization ($|P| < 0.05$) for 160° < ε < 180° (Weinberg 1964, Wolstencroft and Rose 1967, Frey et al. 1974). The color of the zodiacal light is considered to be solar-like (C ≃ 0.9 to 1.1) in the

region $\lambda \simeq 2$ µm to 260 nm for $\varepsilon \gtrsim 20°$ (Nishimura 1973, Hofmann et al. 1973, Frey et al. 1974, Feldman 1977).

Recent observations are now available for directions out of the ecliptic plane (Dumont and Sánchez 1976, Classen 1976, Frey et al. 1974). Intensities reported for the ecliptic pole cluster around 60 S_{10} (Dumont 1979) while the ratio of brightness in the ecliptic to that at the same elongation in the helioecliptic meridian (plane containing both Sun and ecliptic pole) is 3.1 to 3.3 for elongations ε between 15° and 90° (Weinberg and Sparrow 1978).

Topics requiring further investigation include: intensity and color of the zodiacal light at $\lambda < 250$ nm; the zodiacal light in the far infrared region and close to the Sun; a controversy about reported slight circular polarization (≤ 0.005) near the Gegenschein; problems of the deviations ($< 4°$) between the ecliptic and the symmetry plane(s) of the zodiacal light; and slight variations of the rather stable zodiacal light (cf. Dumont 1979 and this volume).

1.4 Integration over the Line of Sight

According to Fig. 1 the flux $\mathrm{I}d\Omega$ of the zodiacal light observable in the direction of the LOS and coming from a spatial angle $d\Omega$ is due to all dust grains in the observer's viewing cone along the LOS. Each volume element $\Delta^2\, d\Omega\, d\Delta$ contributes according to its illumination by the sun ($\sim 1/r^2$) and proportional to the volume scattering function $n\sigma$ ($cm^{-1}ster^{-1}$) of the dust per unit volume contained in the element. Here $n = n(\vec{r})$ is the spatial number density (cm^{-3}) of grains at $\vec{r}$ and $\sigma(\Theta)$ is the (average) differential scattering cross section ($cm^2 ster^{-1}$) per grain in the direction of the scattering angle Θ. Then, after integration over the LOS we obtain (e.g. Leinert 1975)

$$I(L,\beta) = A^2\, F_o\, \int_0^\infty \frac{n(\vec{r})\, \cdot\, \sigma(\Theta)}{r^2}\, d\Delta \tag{5}$$

where $A = 1$ AU and F_o the solar flux (erg $cm^{-2}s^{-1}A^{-1}$) at 1 AU. For simplicity it is usually assumed that σ is independent of $\vec{r}$ and that $n(\vec{r})$ can be separated as for example

$$n = n_o(r/A)^{-\nu}\cdot\exp\left[-\left(\gamma\,\frac{z}{A}\right)^2\right] \qquad\qquad \text{Gauß Model} \tag{6}$$

$$n = n_o(r/A)^{-\nu}\cdot\exp\left[-\,\gamma\sin\beta_\odot\right] \qquad\qquad \text{Fan Model} \tag{7}$$

$$n = n_o(r/A)^{-\nu}\cdot\left[1 + (\gamma\,\sin\beta_\odot)^2\right]^{-\nu/2} \qquad \text{Ellipsoid Model} \tag{8}$$

Here $\beta_\odot = \sin^{-1} z/r$ and n_o is the number density at 1 AU.

If both the observer and the LOS remain in the ecliptic plane, one obtains from (5)

$$I(\varepsilon) = A \, F_o n_o \; \cdot \; (\frac{A}{R \, \cos \, \varepsilon})^{\nu+1} \; _\varepsilon\!\int^\pi \sigma(\Theta) \, (\sin\Theta)^\nu \; d\Theta \tag{9}$$

(For the three dimensional case cf. e.g. Giese 1968, Giese and
v. Dziembowski 1969).

    $I(\varepsilon)$ depends on both $\sigma(\Theta)$ and ν, the increase of number density
towards the Sun. Low values of ν suffice, therefore, for grains
favouring forward scattering for $\Theta \leqslant 90°$. On the other hand, $I(\varepsilon)$
can be approximated by grains which are nearly isotropic scatterers,
if the dust density increases sufficiently. These ambiguities can be
settled by spaceprobes since an instrument that looks always in the
same direction ε_o while the spacecraft changes its solar distance R
records an intensity $I(\varepsilon_o, R) \sim R^{-(\nu+1)}$ (cf. eqn. (9)).

1.5 Inversion

    In some cases the volume scattering function $n(\vec{r}) \cdot \sigma(\Theta, \vec{r})$ can
be obtained directly for special values of Θ. The principle is quite
obvious in the case when an observer looks in the direction of motion
of his spacecraft (Fig. 2). After advancing along the trajectory by
ds, he no longer sees the contribution of dust $dI \sim n \cdot \sigma \cdot ds$ in the
volume element he has just crossed. Therefore the measurable
gradient $|\partial I/\partial s|$ in his viewing direction is proportional to
$n(\vec{R}_o) \cdot \sigma(\Theta=\varepsilon)$, were $\vec{R}_o$ is the location of the observer and ε the
elongation of the viewing direction.
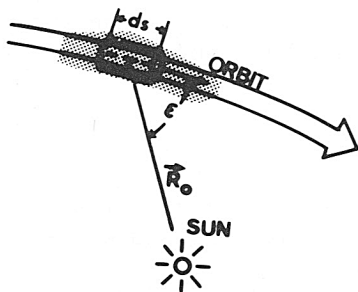

Figure 2
Principle of Inversion

    This "inversion method" was first suggested by Dumont (1972) and
applied to derive $n_o\sigma(90°)$ from groundbased observations (earth's
orbit). Furthermore it can be shown that in the ecliptic plane

$$A^2 F_o \; n(R) \; \cdot \; \sigma(R, \; \Theta=\varepsilon) \; = \; - \, R \cdot \sin\varepsilon \, \frac{\partial I}{\partial \varepsilon} + R^2 \cdot \cos\varepsilon \, \frac{\partial I}{\partial R} \tag{10}$$

and that with the assumption $n \sim r^{-\nu}$ the gradient $\partial I/\partial R$ can be
eliminated (Leinert 1975, Dumont 1976).

Current work is concerned with inversion in the three dimensional case of the forthcoming International Solar Polar (out-of-ecliptic) Mission (ISPM). Here some special directions and the plane determined by the velocity vector and by a vector perpendicular to the helio-ecliptic meridian as seen by the spacecraft ("inversion plane") are of special interest (Schuerman 1979, Dumont et al. 1979, Dumont: this volume).

1.6 Observations from spacecraft

The use of spacecraft provided a big step forward in our knowledge of interplanetary dust:

Rocket photometry of the inner zodiacal light
along circles of constant ($\varepsilon = 15°;21°$) elongation (Leinert et al. 1974) proved, that Gauß-Models and similar layer models can be excluded (Leinert et al. 1976). They are too symmetric close to the sun to be compatible with the observed concentration of the zodiacal light towards the ecliptic plane.

Determination of ν:
Pioneer and Helios observation near the ecliptic plane provide the variation of the brightness as a function of spacecraft location for $0.3\ AU \leqslant R \leqslant 3.5\ AU$ (cf. Weinberg and Sparrow 1978). No appreciable zodiacal light was observed beyond 3.5 AU (Hanner et al. 1976).

From first Pioneer data Hanner et al. (1976) found for a one parameter model $\nu = 1$. From Helios 1 and 2 (Leinert et al. 1978) Leinert (1978) obtains $\nu = 1.3 \pm 0.1$ ($0.09 < r \leq 1\ AU$). This is practically confirmed ($\nu = 1.2$) by inversion of ground based observations by Dumont and Sánchez 1975.

There is currently some debate whether $I \sim r^{-1.3}$ has to be reassessed for $r > 1$ AU and whether particle sizes and/or albedo have to be modi-fied (e.g. Cook 1977, Stanley et al. 1978, Schuerman, this volume).

Volume scattering functions
were derived by Dumont and Sánchez 1975, Dumont 1976 ($\nu = 1.2$), Leinert et al. 1976 ($\nu = 1$), Leinert 1978 ($\nu = 1.3$) and Levasseur-Regourd and Dumont 1978 ($\nu = 1.3$). An example is shown in Fig. 5f (solid curve, $\nu = 1.3$, courtesy C. Leinert).

Sizes of zodiacal light particles:
Dust fluxes derived near 1 AU as presented by Fechtig 1976 were con-verted (assumption: $\rho = 3\ g/cm^3$) by Giese and Grün (1976) into diffet-ential size distributions. It could be demonstrated that the observed values $I(\varepsilon)$ are compatible with the dust fluxes (ibid.: Fig. 2, Leinert et al. 1976: Fig. 6). The main contribution to the zodiacal light (80%) stems from particles about 5 to 100 μm in radius a (see Geise et al. 1978: Fig. 2). A similar result (a = 10 to 100) was obtained by Röser and Staude (1978) using Mie theory.

Out-of-ecliptic International Solar Polar Mission (ISPM)
The ISPM will carry a Photopolarimeter (ZLE), far above (Z = 2 AU) the ecliptic plane which will explore the Z dependence of the zodiacal cloud above the earth's orbit. Multicolor (UV to IR) measurements will allow detection of the general increase of number densities towards the symmetry plane and possible changes in the size distribution, e.g. submicron particles (planetary and/or interstellar) at higher altitude z in the solar system (Greenberg and Schuerman 1978, Giese 1979). Table 1 presents predictions for the intensity $I(R,Z; L,\beta)$ of the zodiacal light expected from a position $R = 1.50$ AU, $Z = 1.48$ AU of the probe above the ecliptic plane where the instrument sees the illuminated cloud below the spacecraft (Fig.3: B) and $R = 1$ AU, $Z = 0.5$ AU where the probe starts reentry into the denser regions of the zodiacal cloud (Fig.3: D). Note that the brightness (e.g. at $L = 30°$, $\beta = 0$) is expected to increase dramatically within a few weeks during descent. Table 1 also demonstrates differences between an ellipsoid and a fan model.
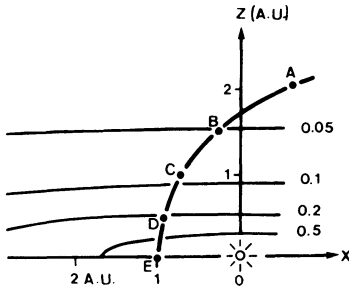

Figure 3
Reentry of the ISPM into the zodiacal cloud.
($\nu = 1.3$, $\gamma = 6.5$, Ellipsoid; parameter n/n_o)
B: 85 days
D: 24 days
before perihelion (E)

Table 1 Zodiacal Light (S_{10}) from ISPM (see text)

Ellipsoid ($\nu = 1.3$, $\gamma = 6.5$); Fan ($\nu = 1.3$, $\gamma = 2.1$)

Z = 1.48, R = 1.50

Ellipsoid βL	0	30	60	90	120	150	180	Fan βL	0	30	60	90	120	150	180
90	5	5	5	5	5	5	5	90	8	8	8	8	8	8	8
60	5	5	5	5	5	5	5	60	7	7	7	7	7	7	7
30	6	6	6	6	6	6	6	30	9	9	9	9	9	9	9
0	13	13	12	12	11	11	11	0	19	19	18	18	17	17	16
-30	54	52	47	41	37	34	33	-30	72	69	62	54	48	45	43
-60	493	415	288	200	152	129	122	-60	644	542	375	260	197	167	158
-90	3180	3180	3180	3180	3180	3180	3180	-90	4200	4200	4200	4200	4200	4200	4200

Z = 0.50, R = 1.05

Ellipsoid βL	0	30	60	90	120	150	180	Fan βL	0	30	60	90	120	150	180
90	17	17	17	17	17	17	17	90	28	28	28	28	28	28	28
60	22	21	20	19	18	19	20	60	35	34	33	31	33	33	34
30	41	36	30	25	24	26	+	30	64	60	51	44	41	44	+
0	242	148	82	57	46	44	45	0	378	240	127	84	65	62	63
-30	+	1120	254	122	83	70	67	-30	+	1360	303	146	100	83	80
-60	410	304	188	130	100	85	81	-60	536	398	240	161	123	105	100
-90	126	126	126	126	126	126	126	-90	159	159	159	159	159	159	159

Z = 0.0, R = 1.0

Ellipsoid βL	0	30	60	90	120	150	180	Fan βL	0	30	60	90	120	150	180
90	63	63	63	63	63	63	63	90	83	83	83	83	83	83	83
60	89	83	74	70	64	61	60	60	121	114	101	91	82	76	75
30	360	222	129	101	84	85	89	30	490	312	173	123	97	96	99
0	+	1800	394	200	141	136	+	0	+	1800	394	200	141	136	+
-30	360	222	129	101	84	85	89	-30	490	312	173	123	97	96	99
-60	89	83	74	70	64	61	60	-60	121	114	101	91	82	76	75
-90	63	63	63	63	63	63	63	-90	83	83	83	83	83	83	83

2.   DUST PROPERTIES FROM SCATTERING

2.1 Consequences of recent observations

The results referred to above rule out earlier models based on dielectric submicron particles with a steep ($\sim a^{-4}$da) size spectrum (Little et al. 1975, Weinberg 1964) and also models of slightly absorbing particles with a flat spectrum ($\sim a^{-2.5}$da) in the half micron and micron size domain (Giese and v. Dziembowski 1969). In both cases the scattering functions required a rather homogeneous spatial distribution ($\nu \simeq 0.1$) and too many small particles compared to the flux curves such as presented by Fechtig 1976. For larger particles there are two approaches to meet the observational facts.

2.2 Mie calculations for large particles

Mie theory (van de Hulst 1957) permits calculation of scattering functions, even for large particles (10 to 100 μm) of both dielectric and absorbing material. Based, however, on the assumption of homogeneous spheres, it must be used with caution. In connection with a thorough study of infrared properties of large grains, Röser and Staude (1978) used the spatial distribution and the size distribution derived from space measurements (1.6) to approximate the visual variation of $I(\varepsilon)$ and $P(\varepsilon)$ by a mixture of dielectric and absorbing materials like obsidian, andesite, olivine, magnetite and graphite. The features of dielectrics and absorbers combine to reproduce $I(\varepsilon)$ satisfactorily over the sky. Polarization, however, is stronger and shows a bump in the backward region which is due to the rainbow effect (cf. their Fig.11a-e). The authors suggest ignoring this feature since it is definitely due to spherical geometry which cannot be expected for interplanetary grains. Laboratory results (cf. 2.3) for micron-sized irregular particles, however, suggest that there are further deviations from Mie theory.

2.3 Particle conglomerates (fluffy particles)

Many samples of extraterrestrial dust grains are aggregates of smaller (<1 μm) particles combined into larger (1 to 10 μm) fluffy particles which appear optically rather black (Brownlee et al. 1976). Following the concept to simulate optical scattering by microwave analog measurements (Greenberg et al. 1961) a 35 GHz-scattering laboratory ($\lambda \simeq 8$ mm) was established at Ruhr-University Bochum (Zerull 1973) which has been extensively used to investigate scattering functions of non-spherical particles (Zerull and Giese 1974, Zerull 1976) and especially of absorbing and dielectric fluffy particles (Zerull et al. 1977, Weiß 1977, Schwill 1979). Although present laboratory measurements are only available for scatterers corresponding in the optical region ($\lambda = 0.5$ μm) to radii of a few microns (a $\leq$ 2.5 μm) the results suggest that the empirical scattering functions of inter-planetary dust can be explained by fluffy particles (Giese 1977,

Giese et al. 1978). Figure 4 shows some typical particles used in our
microwave experiments. The behaviour of the scattering function
i ~ σ(Θ) (van de Hulst 1957) and of the degree of polarization p(Θ) is
shown in Figure 5 as an average over different orientations. Here
m = m_1 - im_2 is the complex index of refraction and α = 2πa/λ the size
parameter of a sphere which has the same volume as the irregular
particle. Figure 5a for comparison shows i(Θ) and p(Θ) as obtained by
Mie theory for absorbing and dielectric spheres of similar size and
refractive index.

Dielectric fluffy particles show rather isotropic scattering
(Figure 5b) for larger (Θ ≳ 70°) scattering angles and no pronounced
polarization. This behaviour - different from Mie calculations - was
also found for (Figure 4a) mixtures of compact, non-spherical
dielectric particles (Zerull and Giese 1974, Zerull et al. 1977). For
compact but absorbing particles (Figure 4b) the scattering function
(Figure 5c) is rather isotropic for Θ ≳ 70° with a slight rise towards
Θ = 180°. Polarization corresponds to Fresnel reflection. If the
particle becomes fluffy (Figure 4c) the scattering function (Figure
5d/e) increases from Θ = 90° towards backward scattering (Θ = 180°) by
a factor of about two. Polarization remains positive. It is lower
than for Fresnel reflection and the maximum is shifted in the direction
towards Θ = 90°. This effect is much more pronounced if the refractive
index is less absorbing (cf. m = 1.65-0.25 i vs. m = 1.45-0.05i).
Scattering functions: See Figure 5.

These laboratory results show remarkably common features with the
empirical scattering functions derived from the zodiacal light
Figure 5f (backward enhancement, position of the maximum of
polarization). The remaining discrepancies might be resolved if one
assumes an additional component of dielectric non-spherical particles
(lowering polarization) and larger particle sizes (isotropy for smaller
scattering angles, increase by the narrow diffraction lobe only at
small Θ). This, however, has to be confirmed by laboratory experiments.

Recent developments add further aspects, which also are related
to conglomerates of small particles. Greenberg and Gustafson (cf.
Greenberg, this volume) suggest from microwave results that purely
dielectric submicron cylinders embedded in dielectric material of
lower index of refraction ("birds nests") could also reproduce the
empirical scattering functions. Furthermore recent experiments in our
laboratory have been concerned with fluffy particles which are built
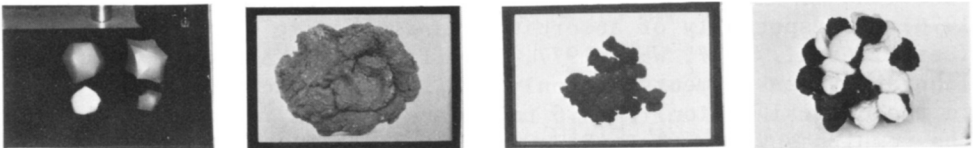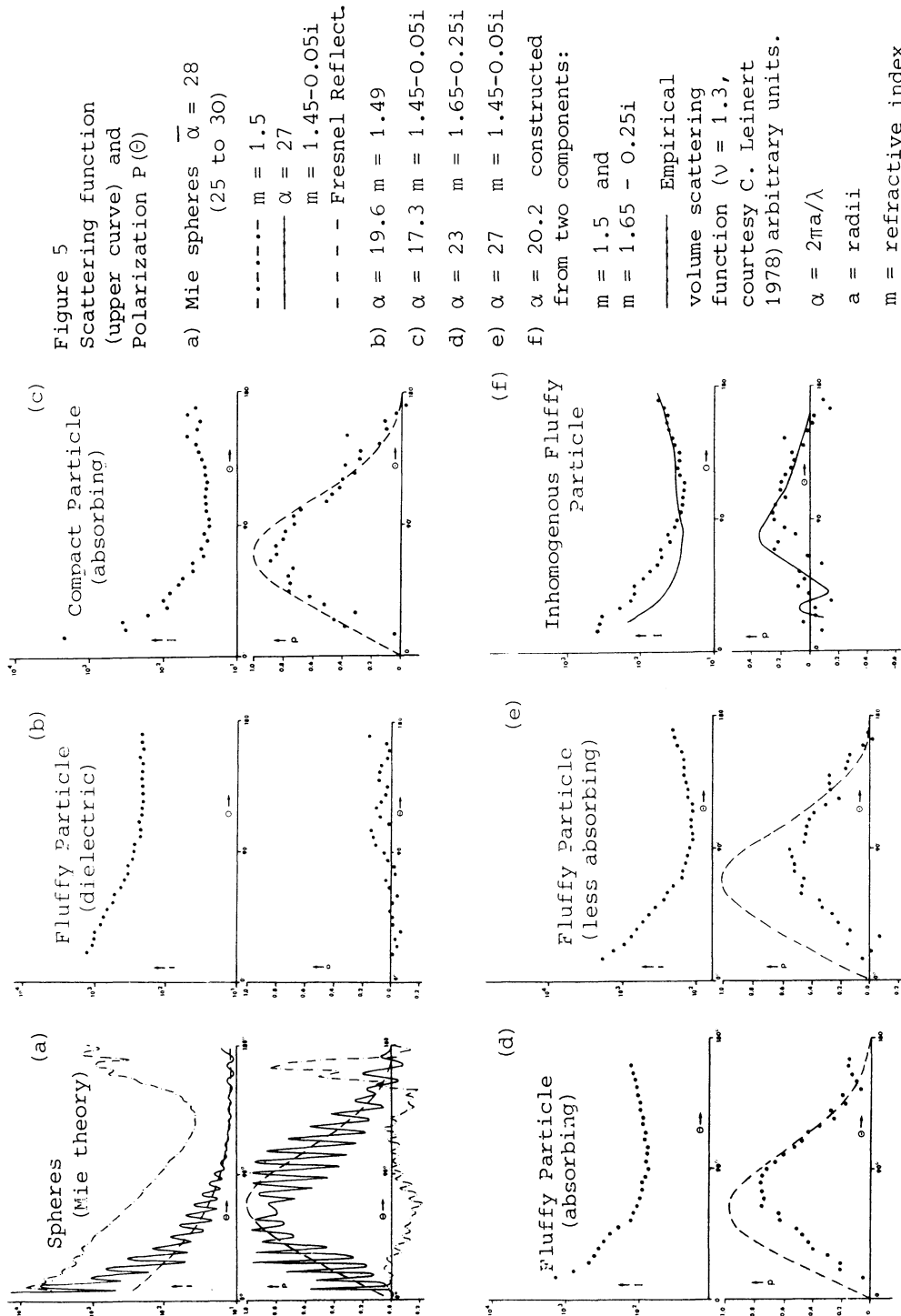up by absorbing and dielectric elements in the same aggregate

Figure: 4a   4b   4c   4d
          Compact particles (4a-4b)   Fluffy particles (4c-4d)

Figure 5
Scattering function
(upper curve) and
Polarization P (Θ)

a) Mie spheres $\overline{\alpha}$ = 28
                 (25 to 30)

   $-\cdot-\cdot-$ m = 1.5
   ——————— α = 27
   $-\cdot\cdot-$ m = 1.45-0.05i
   $-\:-\:-$ Fresnel Reflect.

b) α = 19.6 m = 1.49
c) α = 17.3 m = 1.45-0.05i
d) α = 23   m = 1.65-0.25i
e) α = 27   m = 1.45-0.05i
f) α = 20.2 constructed
   from two components:

   m = 1.5   and
   m = 1.65 - 0.25i

   ———————   Empirical
             volume scattering
             function (ν = 1.3,
             courtesy C. Leinert
             1978) arbitrary units.

   α = $2\pi a/\lambda$
   a = radii
   m = refractive index

(c) Compact Particle
    (absorbing)

(f) Inhomogenous Fluffy
    Particle

(b) Fluffy Particle
    (dielectric)

(e) Fluffy Particle
    (less absorbing)

(a) Spheres
    (Mie theory)

(d) Fluffy Particle
    (absorbing)

(Schwill 1979). These (Figure 4d) inhomogeneous fluffy particles show
lower polarization with a maximum near $\Theta \simeq 90°$ and polarization
reversal at both larger ($\Theta \simeq 160$) and lower ($\Theta \simeq 30$) angles (Figure 5f).
The negative polarization observed in the zodiacal light at large
elongations and the possible negative polarization in the empirical
scattering functions for $\Theta \le 40°$ deserve further attention.

2.4 Application to comets

Recent results from Comet West (Ney and Merrill 1976, Oishi et al.
1977, Isobe 1976, 1978) and other comets (Dobrovolsky et al. 1979) give
some impression about the variation of $\sigma(\Theta)$ and $P(\Theta)$ for cometary dust
over a considerable region of Θ (Figure 6). Using Mie theory, Ney and
Merrill arrive at a typical grain size a $\simeq 1$ μm. This can be confirmed
by comparing $\sigma(\Theta)$ with laboratory results for compact irregular
particles. Furthermore, $\sigma(\Theta)$ and the polarization in the region
$70° \le \Theta \le 140°$ can be reproduced by mixtures of such compact dielectric
and of compact absorbing grains in the micrometer size range (Figure 6).
Inhomogeneous fluffy particles (Figure 5f) show enhanced backward
scattering and in addition to moderate (20 to 30%) positive polariza-
tion for medium scattering angles ($\Theta \simeq 90°$) also negative polarization
($\Theta \ge 150°$) as observed by Dobrovolsky et al. (1979). Therefore, at
least in the visual and near infrared region, irregular and fluffy
particles are a promising alternative to Mie models (cf. Oishi et al.
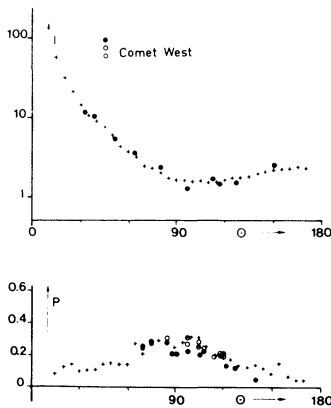1978).

Figure 6
I ~ $\sigma(\Theta)$ Ney and Merrill   •
P   Isobe 529 nm   •
P   Oishi 1 μm   ⊚
P   Oishi 1.25 μm   ○

+   Mixtures dn ~ α^{-k} dα
    irregular compact particles
    60% m = 1.5 − 0.005i
        $1.9 \le \alpha \le 17.8$ k = 2.5
    40% m = $\overline{1.45}$ − 0.05i
        $9.8 \le \alpha \le 17.3$ k = 2

3. CONCLUSION

Optical zodiacal light measurements are still valuable to
determine the three dimensional dust distribution, to separate possible
different size populations, and to investigate in a rather general
way the shape and structure of dust grains. Since scattering effects
are strongly dependent on geometric properties the chemistry of grains

remains the domain of in situ detectors and of infrared investigations. A promising candidate to explain optical properties of both zodiacal light and cometary dust is an aggregate of small particles clumped together to form larger grains.

REFERENCES

Brownlee, D.E., Tomandl, D.A., Hodge, P.W.: 1976, Lecture Notes in
    Physics 48, pp. 279-283.
Classen, Ch.: 1976, 'Eine Blau-Photometrie der Milchstraße und des
    Zodiakallichts', Rheinische Friedrich-Wilhelm Universität Bonn
    (Ph.D. Thesis).
Cook, A.F.: 1978, Icarus 33, pp. 349-360.
Dumont, R.: 1972, C.R. Acad. Sci. Paris 275, Série B, pp. 765-768.
Dumont, R., Sánchez, F.: 1975, Astron. Astrophys. 38, pp. 405-412.
Dumont, R.: 1976, Lecture Notes in Physics 48, pp. 85-100.
Dumont, R.: 1976, Lecture Notes in Physics 48, pp. 115-119.
Dumont, R., Sánchez, F.: 1976, Astron. Astrophys. 51, pp. 393-399.
Dumont, R., Rapaport, M., Schuerman, D., Levasseur-Regourd, A.C.: 1979,
    Space Research XIX, pp. 451-454.
Dobrovolsky, O.V., Kiselev, N.N., Chernova, G.P.: 1979, IAU Commission
    No. 15, Montreal 1979.
Fechtig, H.: 1976, Lecture Notes in Physics 48, pp. 143-155.
Feldman, P.D.: 1977, Astron. Astrophys. 61, pp. 635-639.
Frey, A., Hofmann, W., Lemke, D., Thum, C.: 1974, Astron. Astrophys. 36,
    pp. 447-454.
Giese, R.H.: 1968, ESRO SN-41.
Giese, R.H., v. Dziembowski, C.: 1969, Planet. Space Sci. 17,
    pp. 949-956.
Giese, R.H., Grün, E.: 1976, Lecture Notes in Physics 48, pp. 115-139.
Giese, R.H.: 1977, J. Geophys. 42, pp. 705-716.
Giese, R.H., Weiss, K., Zerull, R.H., Ono, T.: 1978, Astron. Astrophys.
    65, pp. 265-272.
Giese, R.H.: 1979, Astron. Astrophys. 77, pp. 223-226.
Greenberg, J.M., Schuerman, D.W.: 1978, Nature 275, No. 5675,
    pp. 39-40.
Hanner, M.S., Sparrow, J.G., Weinberg, J.L., Beeson, D.E.: 1976,
    Lecture Notes in Physics 48, pp. 29-35.
Hofmann, W., Lemke, D., Thum, C., Fahrbach, U.: 1973, Nature Phys. Sci.
    243, pp. 140-141.
Hulst, van de, H.C.: 1957, 'Light Scattering by Small Particles',
    John Wiley & Sons, New York, London, 1957.
Isobe, S.: 1976, IAU Commission No. 15, Grenoble 1976.
Isobe, S.: 1978, personal communication.
Leinert, C., Link, H., Pitz, E.: 1974, Astron. Astrophys. 30, pp. 411-422.

Leinert, C.: 1975, Space Sci. Rev. 18, pp. 281-339.
Leinert, C., Link, H., Pitz, E., Giese, R.H.: 1976, Astron. Astrophys.
    47, pp. 221-230.
Leinert, C. Hanner, M., Pitz, E.: 1978, Astron. Astrophys. 63,
    pp. 183-187.
Leinert, C.: 1978, 'Die räumliche Verteilung des interplanetaren
    Staubes nach Zodiakallichtbeobachtungen von Helios 1 und 2',
    Ruprecht-Karl-Universität Heidelberg (Habilitationsschrift).
Levasseur-Regourd, A.C., Dumont, R.: 1978, Comptes Rendus des Journées
    de Planétologie, Paris.
Little, S.J., O'Mara, B.J., Aller, L.H.: 1965, Astron. J. 70,
    pp. 346-352.
Ney, E.P., Merrill, K.M.: 1976, Science 194, pp. 1051-1053.
Nishimura, T.: 1973, Publ. Astron. Soc. Japan 25, pp. 375-384.
Oishi, M., Kawara, K., Kobayashi, Y., Maihara, T., Nogouchi, K.,
    Okuda, H., Sato, S., Iljima, T., Ono, T.: 1977, 'Infrared
    Observations of Comet West (1975n) I. Observational Results',
    Kyoto University (preprint) KUNS 112.
Oishi, M., Okuda, H., Wickramasinghe, N.C.: 1977, 'Infrared Observations
    of Comet West (1975n) II. A Model of Cometary Dust', Kyoto Univers.
    (preprint) KUNS 413.
Röser, S. and Staude, H.J.: 1978, Astron. Astrophys. 67, pp. 381-394.
Schuerman, D.W.: 1979, Planet. Sci. 27, pp. 51- 56.
Schwill, S.: 1979, 'Mikrowellen-Analogie-Messungen und qualtitative
    Diskussion zum optischen Streuverhalten loser Partikelkonglomerate
    (Fluffy Particles)' Wiss. Prüfungsamt Bochum (Staatsexamensarbeit).
Stanley, J.E., Singer, S.F., Alvarez, J.: 1979, Icarus 37, pp. 457-466.
Weinberg, J.L.: 1964: Annales d'astrophys. 27, pp. 718-738.
Weinberg, J.L. and Sparrow, J.G.: 1978, in McDonnell (ed.), 'Cosmic
    Dust', John Wiley & Sons, Chichester, New-York, Brisbane, Toronto,
    pp. 75-122.
Weiss, K.: 1977, 'Untersuchungen des Streuverhaltens unregalmäßig
    geformter, absorbierender Partikel mit Mikrowellen', Ruhr-Universität
    Bochum, Abt. Physik u. Astronomie, (Diplomarbeit).
Wolstencroft, R.D., Rose, L.J.: 1967, Astrophys. J. 147, pp. 271-292.
Zerull, R.: 1973, 'Mikrowellenanalogieexperimente zur Lichtstreuung an
    Staubpartikeln', Ruhr-Universität Bochum (Ph.D. Thesis).
Zerull, R.H., Giese, R.H.: 1974, in T. Gehrels (Hrsg.) 'Planets, Stars
    and Nebulae Studied with Photopolarimetry', University of Arizona
    Press, Tucson, pp. 901-915.
Zerull, R.: 1976, Lecture Notes in Physics 48, pp. 130-134.
Zerull, R.H., Giese, R.H., Weiss, K.: 1977, Applied Optics 16,
    pp. 777-778.

DISCUSSION

Feldman: Can you comment on the ultraviolet properties of the fluffy
particles of your models?
Giese: Although the wavelength dependence of the refractive index might
raise additional problems, ultraviolet measurements or simulations

would be extremely helpful to distinguish between different polarization mechanisms for differing particle structures, e.g. shadowing and Fresnel reflection (large fluffy particles) vs Rayleigh-like scattering for small needles (birds nests). I would expect the latter to be more sensitive to decreasing wavelength.

Leinert: Will you extend the scattering measures to larger particles?
Giese: Yes, the equipment will soon be ready to do laser scattering experiments on electrically suspended single particles of 10 to 100 μm size.

Stanley: Cook (1978) developed a mass flux curve which fits the in situ data. How would this curve fit the zodiacal light data and what does this suggest about the assumptions made in comparing the data?
Giese: Cook used a bulk density of 0.18 g/cm^3 but if we use a density of 0.38 the brightness increases 4 times which allows use of a low albedo.